JOURNAL OF GEOPHYSICAL RESEARCH, VOL. 95, NO. B4, PAGES 4857–4872, APRIL 10, 1990

Right-Lateral Displacements and the Holocene Slip Rate Associated With Prehistoric Earthquakes Along the Southern Panamint Valley Fault Zone: Implications for Southern Basin and Range Tectonics and Coastal California Deformation

PEIZHEN ZHANG, MICHAEL ELLIS, D. B. SLEMMONS, AND FENGYING MAO

Center for Neotectonic Studies, University of Nevada, Reno

The N20°W-trending Panamint Valley fault zone is linked to the N60°W-trending Hunter Mountain strike-slip fault and the Saline Valley fault system, which represents one of the three major fault systems accommodating active crustal extension in the southern Great Basin. A 25 km-long zone of fault scarps along the southern Panamint valley fault zone is recognized as the surface rupture zone associated with the most recent prehistoric earthquake. The displacement associated with the most recent event, determined through six detailed topographic maps of offset features, is 3.2 ± 0.5 m, and a number of larger offsets, in range of 6–7 m and 12 m, are also observed. If the larger displacements represent, respectively, two and three events, each of ~3 m, then the fault zone appears to be associated with a characteristic earthquake, which we estimate from the length of the rupture zone and the displacement to be between (Ms) 6.5 and 7.2. The Holocene slip rate is 2.36 ± 0.79 mm/yr, is determined from the displacement of two alluvial features whose maximum age is estimated from pluvial shorelines. Assuming a characteristic earthquake model, the recurrence interval is between 860 and 2360 years. The Holocene slip rate appears to be similar to the 4 million year slip rate of 2–2.7 mm/yr (determined from the Hunter Mountain fault), which we suggest reflects the relatively constant tectonics in this region over the last 4 million years. We further speculate that this supports the San Andreas discrepancy in that the Holocene slip rate of the San Andreas fault probably represents its very-long term (several Ma) slip rate. The total slip vector of the southern Panamint Valley fault system is oriented toward ~N35°W, making this a predominantly strike-slip fault. In conjunction with the N60°W orientation of the Hunter mountain strike-slip fault, we suggest that the displacement vector for the southern Great Basin is toward the NW, consistent with results from VLBI data, rather than WNW as determined by combining VLBI and geological data. This in turn suggests that the coastal California deformation component involves, respectively, less shortening and more strike-slip displacement perpendicular and parallel to the San Andreas fault than is currently proposed.

INTRODUCTION

This paper describes the paleoseismic right-lateral displacement and the Holocene slip rate of the Panamint Valley fault system. We also attempt to place the character of the fault system within the context of the regional modern deformation, although a fuller treatment of the regional neotectonics will be presented in another paper.

Panamint Valley is within the Death Valley Extensional Region (Figure 1), the most active part of the Southern Basin and Range Province during late Neogene and Quaternary time. This very active extensional region includes the ENE-trending Garlock fault, and the NNW-trending Owens Valley, Panamint Valley, and Death Valley fault zones. Geomorphic evidence suggests that the region continues to very active, although historically it is seismically quiet. North of the left-lateral Garlock fault, the region is characterized by a combination of range-front and alluvial fan-cutting fault systems, which appear to have dominantly normal and right-lateral strike-slip sense of motion, respectively.

Neogene tectonic development of the region has been described by a number of workers since the pioneering work of *Noble* [1941] (see, *Wernicke et al.* [1988*a*, *b*, and 1989] for a more detailed review). There is general agreement that the region comprises a series of east-tilted blocks of mainly lower Paleozoic miogeoclinal units, separated from each other by late Neogene and Quaternary alluvial and lake sediments. Estimates of Tertiary extension are currently under debate, although good evidence from displaced Mesozoic thrusts and lower Paleozoic unconformities [*Wernicke et al.*, 1988*a*, *b*], and displaced lower Paleozoic isopachs [*Stewart*, 1978, 1983], suggests extension values up to a maximum of 300 km (300%), in a west-north-west direction [*Wernicke et al.*, 1988*a*, 1988*b*]. The southern Basin and Range Province is also thought by many workers to have extended, and to be currently extending, along low-angle normal faults [e.g., *Burchfiel et al.*, 1987; *Hodges et al.*, 1989; *Wernicke et al.*, 1988*a*, *b*, 1989].

Our preliminary geomorphic and paleoseismic analysis of the region suggests that the most recent tectonic activity is within Death Valley, Panamint Valley, and Owens Valley (Figure 1), although probable Quaternary fault scarps are also evident in Pahrump Valley and Amargosa Valley further east. The topography of the region and the range-hugging nature of much of the fault system is indicative of dip-slip faulting. Northern Death Valley and its extension, Fish Lake Valley, are also dominated by signs of modern strike-slip motion [*Brogan*, 1979; *Sawyer*, 1989], and this paper describes a similar result from southern Panamint Valley, where the fault system is otherwise a typical range-front type with modern playa sedimentation immediately adjacent to the fault bounded range.

Paper number 89JB03315.
0148-0227/90/89JB-03315$05.00

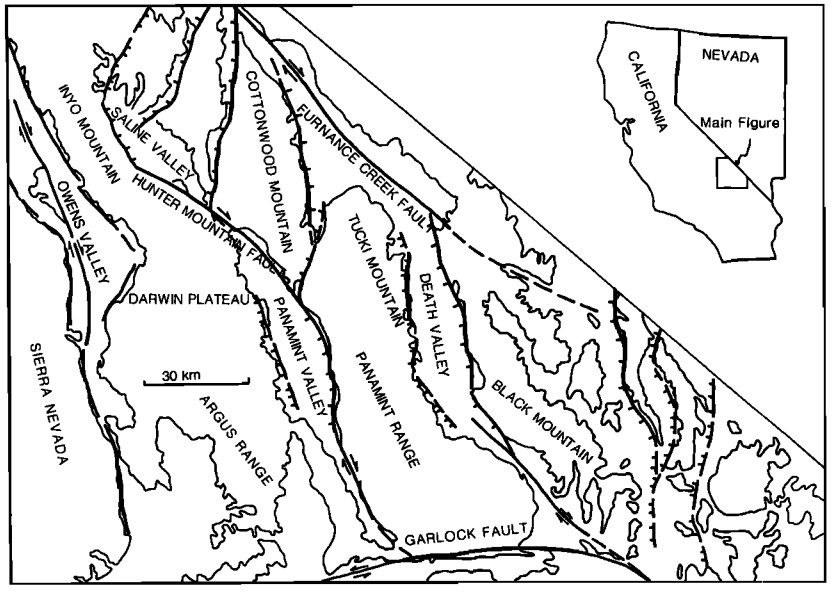

Fig. 1. Major active faults of the Death Valley Extensional Region (modified from *Burchfiel et al.* [1987]). Thick lines with ticks indicate normal faults. Thick lines with arrows indicate strike-slip faults.

Panamint Valley

The geology of Panamint Valley has been described most recently by *Burchfiel et al.* [1987], *Hodges et al.* [1989], and *Schweig* [1989], and the late Pleistocene pluvial history by *Smith* [1976, 1978]. Basin development is thought to have begun with the eruption of late Miocene to Pliocene basalts that now face each other on opposing flanks in the northern part of the valley [*Burchfiel et al.*, 1987; *Hodges et al.*, 1989; *Larsen*, 1979; *Schweig*, 1985, 1989; *Sternlof*, 1988]. K-Ar dates of the basalts from both sides of the valley yield age-estimates of 7.7 to 4.0 Ma [*Hodges et al.*, 1989; *Hall*, 1971; *Larsen*, 1979; *Schweig*, 1989; *Sternlof*, 1988].

The modern day Panamint Valley fault system extends from the Hunter Mountain strike-slip fault, in the north, along the western side of the southern Cottonwood Mountains and Panamint Range, over a central valley topographic high, marked by the Wildrose graben, and quits the Valley to the south through Warm Sulphur Spring Gap (Figure 2). Along the central part of the Valley, with the exception of the Wildrose graben (Figure 2), the fault complex appears to be a typical range-front dip-slip system. In support of this, the modern south playa is also hugging the range-front, indicative of active and relatively high subsidence rates adjacent to the fault, and therefore of a partially dip-slip fault. To the south of the Valley, as we will describe below, the fault system is characterized by dip-slip range-front faults and by strike-slip, alluvial fan-cutting faults.

The Panamint Range and Darwin Plateau (Figure 1) probably stood at essentially the same elevation 4 m.y. ago and were covered by a continuous sequence of basalts, whose upper part is about 4.0 m.y. old, prior to the onset of extension [*Sternlof*, 1988]. The basalts capping both the Panamint Range and Darwin Plateau are chemically identical [*Walker and Coleman*, 1987]. Magnetic survey profiles across the valley suggest that the basalts, abundant on either side of the valley, are absent from beneath as much as 9 km of the width of the valley floor [*MIT 1985 Field Geophysics Course and Biehler*, 1987]. This suggests that the inception of opening was probably after formation of the 4 m.y.-old basalts, otherwise the basalts would fill the valley. The northern part of the valley may be underlain by an active low-angle normal fault dipping gently toward the northwest, and adjacent to the Hunter Mountain strike-slip fault [*Burchfiel et al.*, 1987; *Hodges et al.*, 1989; *MIT 1985 Field Geophysics Course and Biehler*, 1987; *Sternlof*, 1988]. The offset (9.3 ± 1.4 km) of a well-defined 4 m.y. old piercing point across the Hunter Mountain fault yields a minimum slip-rate of 2–2.7 mm/yr [*Burchfiel et al.*, 1987]. *Schweig* [1989], however, suggests that the valley opened about 6.1 m.y. ago, and if this is correct, the minimum slip rate would be 1.30–1.75 mm/yr.

The seismicity of Panamint Valley has been low during historic time. Maps of earthquake epicenters during 1900–1976 [*Hileman et al.*, 1973; *Real et al.*, 1978; *R. B. Smith*, 1978] show sparse events in the region, and no large events occurred in the valley. *Richter* [1958] assigned the M = 6, November 4, 1908 earthquake to the southern Panamint range, although the absence of building damage and modern surface rupture does not support this location [*R. S. U. Smith*, 1979].

R. S. U. Smith [1979] first reported Holocene faulting along the Panamint Valley fault zone, between Ballarat and Goler Wash canyon, and pointed out that the most recent offset probably occurred at several hundred years ago. The purpose of this paper is to describe the right-lateral displacement and the present evidence for the Holocene slip rate along the southern Panamint Valley fault zone. We will first describe the active fault system in the southern part of the valley. Fault maps, produced through field work and analysis of low-sun angle aerial photography, are presented, as well as detailed topographic maps of selected Holocene offsets.

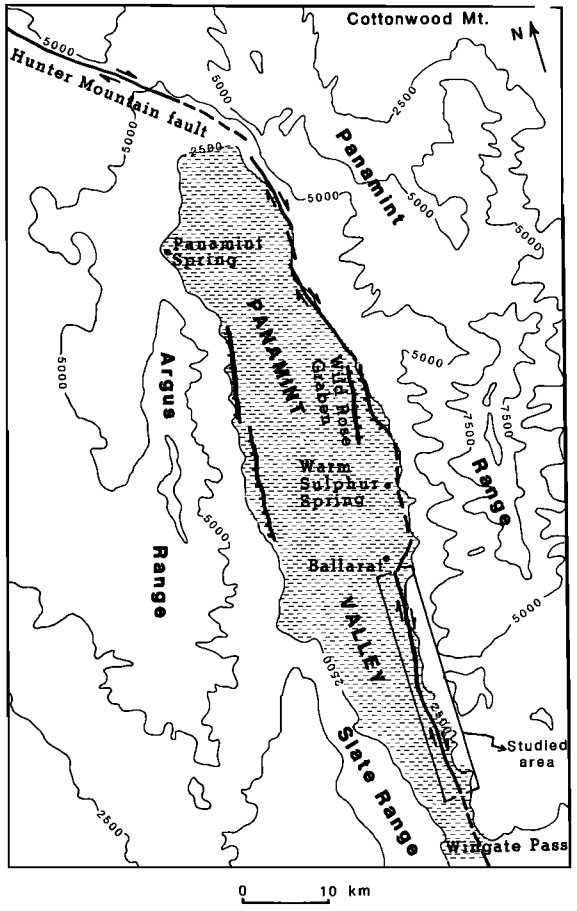

Fig. 2. Major active faults within Panamint Valley. Thick lines are the active faults. Arrows indicate the sense of motion and ticks indicate dips of the faults.

PREHISTORIC SURFACE RUPTURE AND ASSOCIATED DISPLACEMENT

A 25 km-long zone of fault scarps extends along the eastern side of southern Panamint Valley, from Goler Wash Canyon northward to Ballarat (Figures 2 and 3), and trends approximately N10W to N30W. There are generally two sets of scarps, easily distinguishable on aerial photographs and in the field, one of which is a range-front system *sensu stricto*. The second is parallel to the range and generally cuts the alluvial fans. They both are thought to be associated with the last prehistoric surface rupture because they are generally less vegetated, the slope appears less degraded, and there is little to no development of desert varnish when compared to other nearby fault scarps in the same valley which are of similar relief, in similar host maternal, and share the same climate and environmental factors.

The age of the most recent fault scarps is difficult to estimate. It may be argued that given their fresh appearance and their low relief these scarps must be relatively young, or they would be considerably eroded. This argument is made partly by experience with fault scarps in the Basin and Range Province where degradation of both larger and similarly-sized scarps, for which age-estimates are available, has rendered them almost indistinguishable in the space of hundreds or even tens of years [*Slemmons*, 1957; *Bell et al.*, 1984; *Slemmons et al.*, 1989; *Zhang et al.*, 1989].

The southern end of the rupture zone is not well defined yet because of the coverage of modern alluvial fans. The southernmost observed rupture zone is located near Goler Wash Canyon (Figure 3), and comprises a discontinuous range-front fault, a 3 km long continuous distal-fan fault, and a short, about 1 km, median-fan fault. The western, distal-fan fault strand is almost purely strike-slip, and faces to the west with the western side dropped down, but the fault-dip must be very steep because about 200 m to the north the same scarp faces east. A minimum right-lateral offset is shown to be about 3 m. The short median-fan fault is also almost purely strike-slip and shows right-lateral displacement of about 1 m, bringing the total to about 4 m. The range-front fault dips to the west with its western side dropped down, and the scarp varies in height from 0.4 to 1.2 m. No lateral displacement has been observed along the range-front fault.

Between Coyote Canyon and Manly Peak Canyon the southern Panamint fault system is essentially one fault that hugs the range and trends about N30W (Figure 3), and shows almost purely strike-slip offset. The fault dip is probably steep, because the scarp faces both eastward and westward along its 3 km length. The maximum offset observed in this section is about 60 m.

Along the section of the fault near the mouth of Manly Peak Canyon, where the range-front changes trend slightly toward N10W, the single fault splits into two parts: a typical range-front normal fault and a fan-cutting strike-slip fault about 200 m away from the range-front. Near Manly Peak Canyon, the fan-cutting fault dips steeply toward the east and the scarp height is less than 0.4 m This section of the fault cuts through variously-aged parts of the alluvial fan, and displacements vary from 3 to 30 m. The minimum amount of offset is consistently about 3 m (see sites 3 and 4). The range-front fault shows no lateral displacement.

This strike-slip—range-front pair continues northwards to Manly Fall, where the strike-slip fault ends, and the range-front normal fault continues along the base of the Pleistocene Lake terrace to form a scarp 0.8 to 1.4 m in height.

Between Big Horn Canyon and South Park Canyon the range-front and fan-cutting faults are discontinuous. We have not been able to find any unequivocal lateral offsets on the range-front fault. Only one right-slip offset, 2.6 ± 1 m, is observed along the fan-cutting fault, but we believe it is dominated by strike-slip because the modern alluvium obscured and even destroyed most of the evidence of faulting and displacement.

Near South Park Canyon the range-front fault shows predominantly vertical displacement. The fan-cutting fault is about 200 to 300 m west of the range-front fault and faces east. The modern alluvial fans significantly obscure the fault scarps so that the scarp itself is difficult to recognize in many places. The sense of motion along this fan-cutting fault is still dominated by right-lateral slip as indicated by 4 stream offsets.

At Ballarat the range-front fault is delineated by west-dipping normal fault scarps, and the fan-cutting fault is probably buried beneath the modern playa. Beyond Ballarat, the prehistoric fault trace can not be found on the ground, thus the total apparent minimum length of the most recent prehistoric surface rupture is about 25 km.

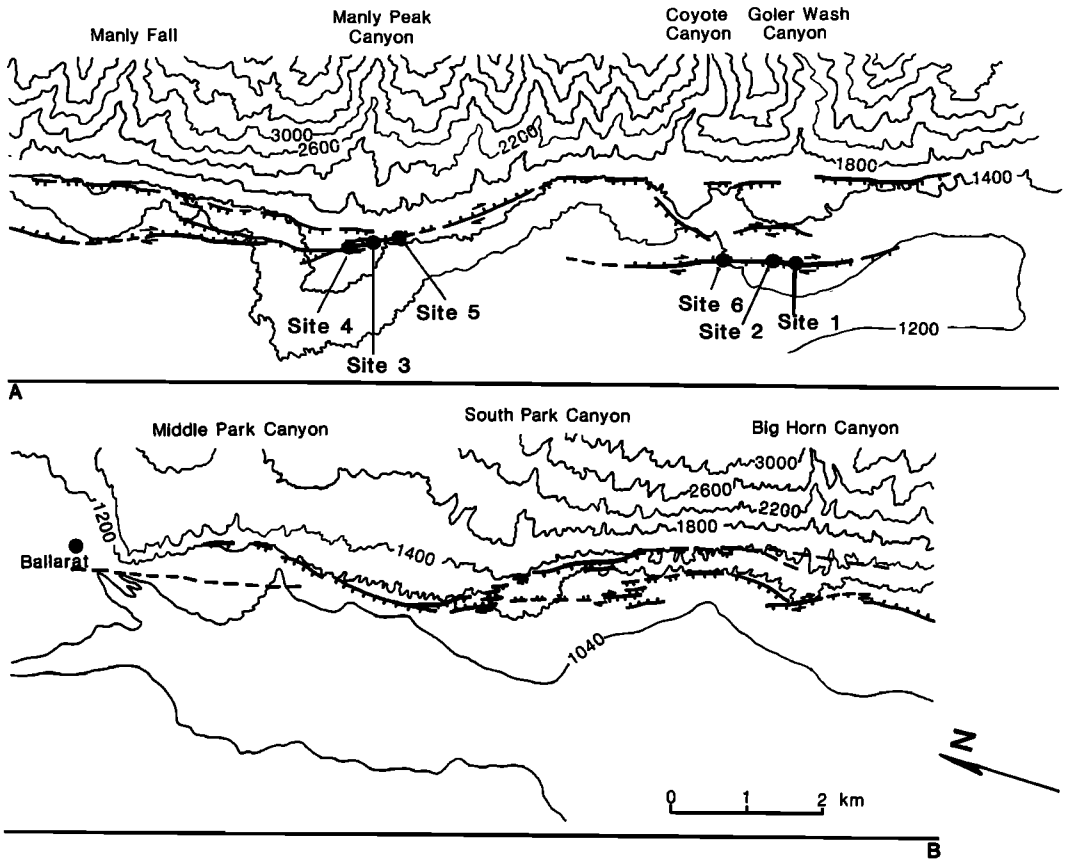

Fig. 3. Geometry of the surface rupture associated with the last prehistoric earthquake between Ballarat and Goler Wash Canyon along the southern Panamint Valley fault zone. The lower panel in the figure lies north of the upper one, and point B is northward continuation of point A. Ticks indicate dips of fault scarps, and arrows indicate sense of lateral displacement. Locations of plane table mapping are also shown on this map.

Details of Prehistoric Displacements

The concept of a meaningful average earthquake recurrence interval [e.g., *Wallace*, 1970] is based on the assumption that the amount of slip that occurred during the past earthquake will recur in a future earthquake, with the interval between them equal to that amount of slip divided by the long-term average rate of slip in the absence of fault-creep. To study the earthquake history, therefore, requires relatively accurate knowledge of the amount of displacement associated with historic or prehistoric earthquakes. In the following sections we describe the details of the offset topographic features at four places along the fault system, which we believe are associated with the most recent prehistoric rupture. In all cases, detailed maps were made using a plane table and alidade, following the methods of *Sieh* [1978] and *Zhang et al.* [1987].

Site 1. Site 1 is located about 1.5 km west of Goler Wash Canyon, and about 200 m south of the dirt road from Panamint Valley to Goler Wash Canyon (Figure 3). The prehistoric surface rupture is marked by a N30W-trending and southwest-facing fault scarp whose height varies from 0.1 to 0.4 m. A series of stream channels and alluvial features (both erosion and deposit) have been offset where they cross the fault scarp. At Site 1, the least amount of offset is measured to be about 3.3 ± 0.4 m by matching the youngest stream channel across the fault scarp (Figure 4). This youngest stream channel, as indicated by the thin dashed line in Figure 4, is 0.3–0.4 m in width and 0.1–0.2 m in depth, and is incised into the bottom of the large channel, whose width is 3–4 m, and whose bed is relatively flat.

The large channel is also offset across the fault scarp, but its geometry is more complex than that of the youngest channel. The northeastern bank of the upstream channel curves northward near the fault scarp (Figure 4), which we interpret as a post-displacement stream undercutting feature. The downstream channel is complicated by another channel about 8 m from the fault scarp. If we ignore these modifications, both the downstream and upstream channel are the same size, and the offset is 6.0 ± 1.0 m. This amount of offset is supported by another offset feature. The southern bank of the large channel is well preserved along both upstream and downstream sections, and is clearly marked by a low scarp that comprises large boulders and cobbles (Figure 4). The amount of displacement on this bank is 5.7 ± 0.5 m, which is about the same as that of the large stream channel.

One can argue that this about 3 m displacement may be a deflection caused by the 5.7 m offset of the old southern bank of the large channel. However, the about 3 m offsets on stream channels and debris flows are observed in many places along this section and close to this site. It is unlikely that this site was not also subject to the 3 m displacement associated with the most recent event. Offset of the large channel and its southern bank (6.0 ± 1.0, 5.7 ± 0.5 m) is

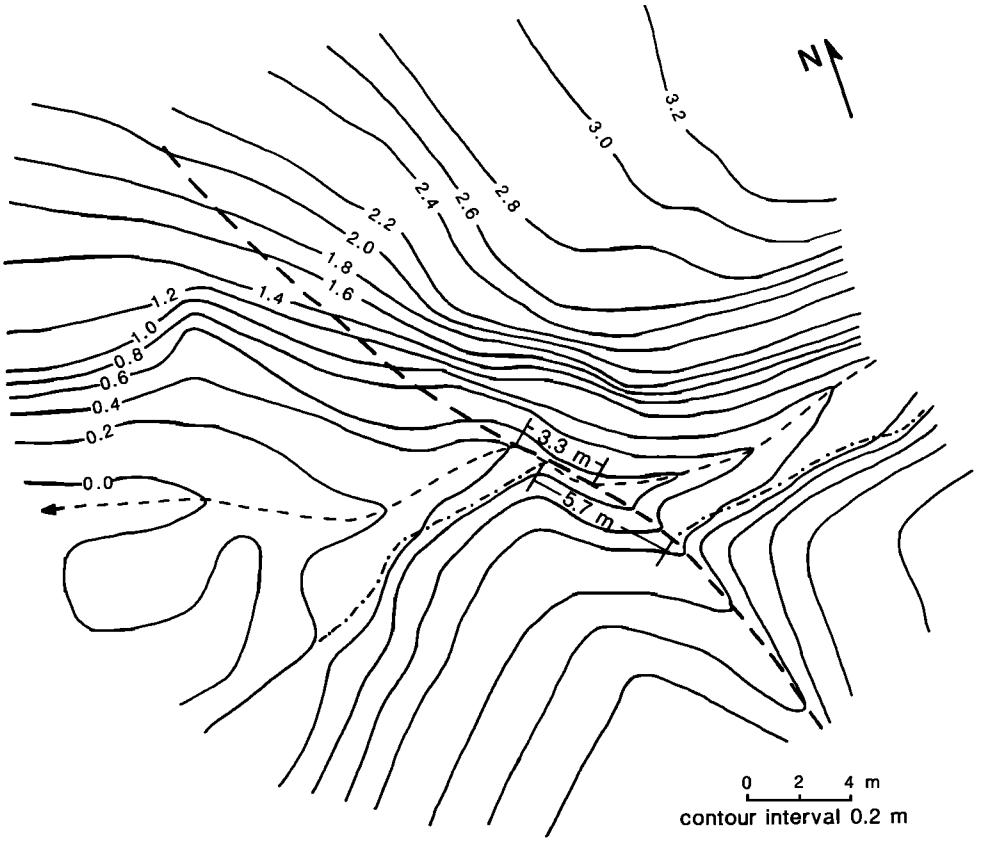

Fig. 4. Topographic contour map of stream offset near Goler Wash Canyon (Site 1). Thick dashed lines indicate fault scarps. Thin dashed lines represent central lines of current stream. Dashed and dotted lines are southern banks of downstream and upstream channels. The measured right-lateral displacement is 3.3 ± 0.4 m between the central lines of the current stream, and is 5.7 ± 0.5 m between the southern channel banks. The elevation is arbitrary.

approximately twice that of the small stream offset (3.3 ± 0.4 m), which suggests two similar offset events.

Site 2. Site 2, 30 m north of Site 1, is also located on the alluvial fan west of Goler Wash Canyon. The N30W-trending and southwest-dipping fault scarp is clearly present on the ground. The stream channel shown in Figure 5 is offset where it crosses the fault. The upstream channel is 5 to 6 m wide with a relatively flat bottom. Two small stream channels are present on upstream channel bottom. The northern one extends only about 12 m in the upstream direction, and the southern one can be followed several tens of meters upstream. Current discharge is carried by both channels. The southern stream flows to the west and turns to the north along the fault and then enters the downstream channel. The northern stream flows directly across the fault into the downstream channel. We suggest that the southern stream channel used to flow directly into the downstream channel, and that it has been offset to its present position during the most recent prehistoric event. The northern stream channel was probably formed after the most recent offset event and has not been subjected to any displacement. The southern upstream channel shows 3.37 ± 0.6 m right lateral offset from the downstream channel. Both banks of the large channel are also offset. If we project appropriate contours to the fault from both sides, they yield the similar amount of displacement (Figure 5).

Site 3. Site 3 is on the alluvial fan near Manly Peak canyon (Figure 3 and 6), about 5.3 km north of Goler Wash canyon. The prehistoric surface rupture zone is characterized by a prominent east-facing fault scarp. The sense of offset on this scarp is dominantly right-slip.

Two minor upstream channels (A and B) are present inside the flat bottom of a large channel (Figure 6). Discharge in channel A flows directly into downstream channel D, and channel B is truncated by the fault scarp. The discharge in channel B turns northwest along the fault scarp, then to the west across the fault and into downstream channel D. Downstream channels C and D both flow into the main channel E far away from the fault, but most present discharge from upstream channels A and B flows into channel D, and only a small amount of discharge flows into channel C. Thus downstream channel C is essentially an abandoned channel (Figure 6). We suggest that upstream channel A used to flow into downstream channel C because channel D looks young and shows evidence of recent strong incision. The right-lateral offset between upstream channel A and downstream channel C is 3.0 ± 0.6 m, which is consistent with about 3 m offset associated with the last offset event.

The southern bank of the large channel also shows displacement. For example, contours 1.6, 1.8, and 2.0 have been offset about 6–7 m (Figure 6), approximately two times the 3 m offset event. The present steep bank represented by contours 1.6, 1.8, and 2.0 is 3.7–4.2 m from the downstream channel E where there is a relatively flat terrace. This terrace was probably formed by eroding the material that used to be part of the downstream channel bank. After the formation of

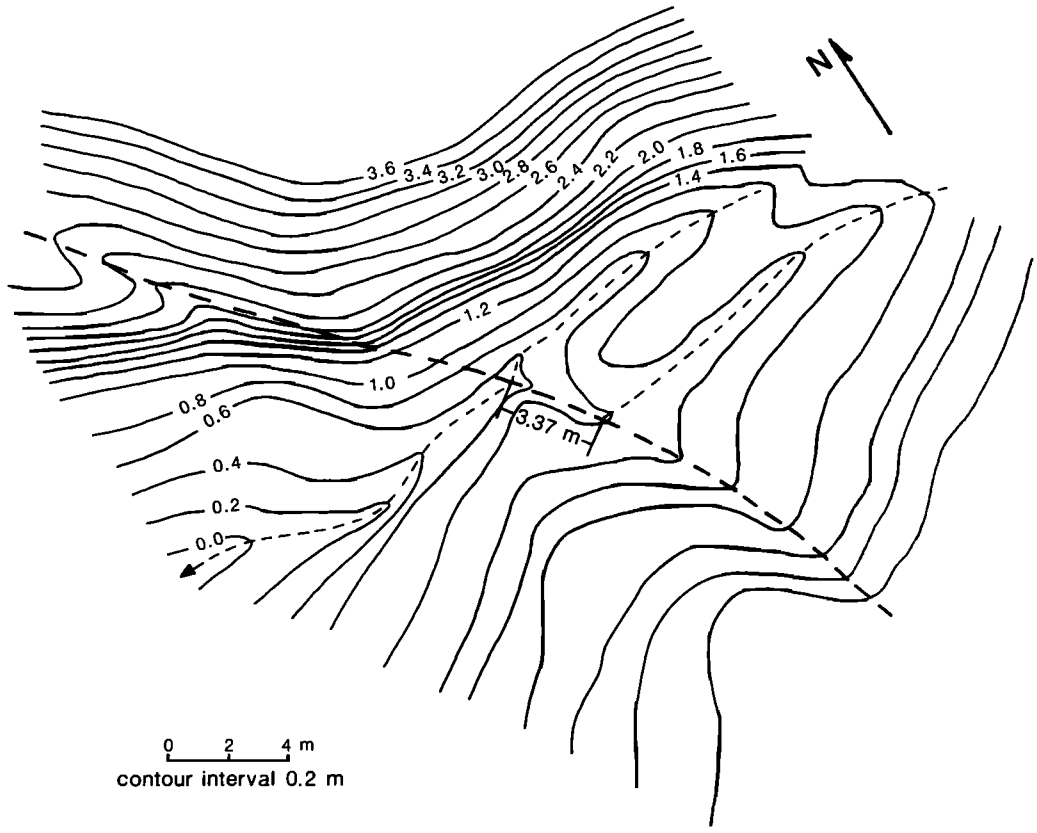

Fig. 5. Topographic contour map of stream offset near Goler Wash Canyon (Site 2). Thick lines represent fault scarps. Thin dashed lines represent central lines of stream channel. The single arrow indicates the direction of stream flow. The measured right-lateral offset between upstream and downstream channels is 3.37 ± 0.6 m. The elevation is arbitrary.

this terrace another two offset events might have occurred and the new channel bank has been offset 6–7 m.

The northern bank of the channel is complex. The downstream channel bank (represented by contours 0.4, 0.6, 0.8, and 1.0) is well defined and hugs the stream (Figure 6). A well-defined terrace is present between the upstream channels A and B. The area northwest of the upstream channel A near the fault (Figure 6) is due to recent channel undercuts. If we ignore this recent undercut area, the northern upstream channel bank should be close to the channel A, and the displacement of the northern channel bank is about 6 m. Moreover, the restored large upstream channel (by ignoring the undercut area) has a size comparable to that of the downstream channel. This offset morphology yields 6–7 m right-lateral displacement.

The upstream channel B is a major channel that can be followed several hundred meters upstream. Upstream channel A developed on the terrace north of channel B, and its total length is only 25 to 30 m. Thus, the upstream channel B is older than the upstream channel A and also than the terrace between A and B. This is supported by the observation that the northern bank of the upstream channel appears to be more freshly eroded than the southern bank of upstream channel. The southern bank of the downstream channel E also appears to be more freshly eroded than the northern bank, and the terrace between channel E and the southern bank is younger than channel E itself. We suggest that the northern bank of the upstream channel was originally adjacent to upstream channel B, the southern bank of downstream channel was originally adjacent to downstream channels C and E, and they were later eroded back to their current position. Thus, the upstream channel B was tectonically displaced from the downstream channel C. The offset is 11.0 ± 2.0 m, which is inferred to be the result of several events (three to four), possibly each of similar size as the most recent one.

Site 4. Site 4 is about 50 m north of Site 3 along the same surface fault trace (Figure 3). At Site 4 only one stream flows from east to west across the fault scarp. 3.1 ± 0.4 m right-lateral offset is obtained by matching upstream and downstream channels along the fault (Figure 7). This offset was probably associated with the most recent prehistoric offset event because the size of the stream is small and its age is probably young. The banks of the channel, especially the southern one, is also offset. If we project the same contour along the general trend of the bank to the fault scarp from both upstream and downstream sides, the offset is approximately 3 m.

Summary of Prehistoric Offset Data

The smallest offsets observed from the four sites are 3.3 ± 0.4, 3.37 ± 0.6, 3.0 ± 0.6, and 3.1 ± 0.4; the average amount associated with the most recent event is 3.2 ± 0.5 m. Along this part of the fault zone about 3 m offset is consistently observed, with the exception of near Goler Wash Canyon

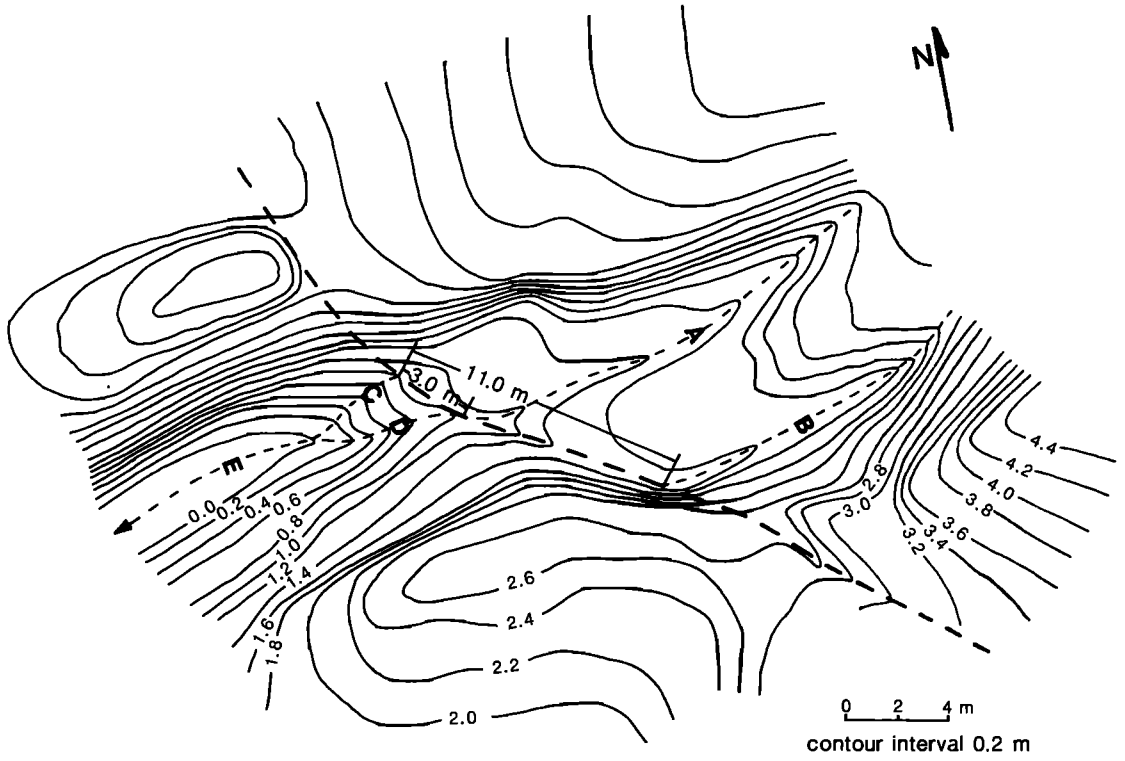

Fig. 6. Topographic contour map of stream offset near Manly Peak Canyon (Site 3). Thick lines represent fault scarps. Dashed lines represent the central lines of stream channels. Single arrow indicates direction of stream flow. A, B, C, D, and E are channels mentioned in the text. The right-lateral displacement is 3.0 ± 0.6 m between upstream channel A and downstream channel C, and is 11.0 ± 2.0 m between downstream channel C and upstream channel B. The elevation is arbitrary.

where the offset may be as large as ~4 m. The 4 m offset may be a reflection of a nonuniform slip distribution, although we see no other signs of such nonuniformity. Alternatively, the short median-fan fault and its 1 m offset may be superficial and confined to the near surface. We do not consider anomalous slip significant since we do not observe it elsewhere. If the about 3 m offset is due to accumulation of two or more offset events, we would expect to see evidence of a smaller offset, which we do not observe. The well-defined morphology of offset features suggest that fault creep has not contributed significantly to the offset, which is further supported by the fact that there is no observed example of fault creep in the Basin and Range Province. Thus the 3.2 ± 0.5 m displacement is probably the average amount of displacement associated with the most recent prehistoric earthquake.

At Sites 1 and 3, and elsewhere along the fault zone, we have observed larger offsets (Figure 4 and 6). We believe these larger displacements were due to the cumulative effect of 2 or more previous events. It is interesting to notice that the 6.0 ± 1.0 m and the 5.7 ± 0.5 m offsets measured at Site 1, and the 6–7 m offset at Site 3, are about twice the average amount of offset associated with the most recent offset, and the 11.0 ± 2.0 m offset at Site 3 is about 3 or 4 times as large as the last event. These data suggest that a number of offset events have occurred along the southern Panamint Valley fault zone, and that at least the past two events each involved about 3 m right-lateral displacement. The 11.0 ± 2.0 offset may be the result of three or four 3-m-events, but other interpretations are also possible. The data are thus consistent with the characteristic earthquake model of *Schwartz and Coppersmith* [1984, 1986].

We may estimate the magnitude of the most recent earthquake through use of rupture-length and displacement vs. magnitude relationships [*Slemmons et al.*, 1989]. The observed length of the rupture zone associated with the most recent event is about 25 km. This is a minimum length, because both southern and northern ends are covered by modern sediments. The length is probably not much longer than 30 km, because the fault scarp is not found beyond the modern alluvial fan and playa deposit to the northern and southern ends. Thus, giving a rupture-length of 25 km and 3 m displacement, the magnitude of the characteristic earthquake along the Southern Panamint Valley fault zone would be 6.5–7.2 (Ms).

HOLOCENE SLIP RATE

The Holocene slip rate of an active fault may be determined by dating offset landforms. Dating such landforms, however, is usually difficult, and there are few faults for which accurately dated offset landforms have been used to determine Holocene or late Pleistocene slip rates [e.g., *Sieh and Jahns*, 1984; *Weldon and Sieh*, 1985]. The maximum or minimum slip rate can be estimated for a certain displacement if the relation of such displacement to a known-age landform or geomorphic surface can be obtained [*Zhang et al.*, 1988]. We have used this method to estimate the minimum slip rate during the Holocene and late Pleistocene along the southern Panamint Valley fault zone.

Fig. 7. Topographic contour map of offset stream near Manly Peak Canyon (Site 4). Thick lines represent fault scarps. Dashed line represent the central line of the stream channel. The right-lateral displacement is 3.1 ± 0.4 m by matching up central lines between upstream and downstream channels. The elevation is arbitrary.

Panamint Valley was occupied by a pluvial lake during the late Pleistocene and the earliest Holocene [*R. S. U. Smith*, 1976; also Pluvial history of Panamint Valley, California, unpublished guidebook, Friends of the Pleistocene, 1978]. Lake Panamint was subjected to five stages of fluctuation. From oldest to youngest these are named the E, F, G, H, and I stages [*R. S. U. Smith*, 1976; also unpublished guidebook, 1978]. During each fluctuation time the lake stood at 2000 feet above sea level and was maintained at this level by overflow of water from Panamint Valley to Death Valley. After the last high stand of Lake Panamint, during I-stage, the lake started to dry. Shorelines below 1200 feet represent the last low stand 13,000 to 12,000 years ago [*R. S. U. Smith*, 1976; also unpublished guidebook, 1978]. The age estimation of the five stages of fluctuation are based on several radiocarbon dates and the assumption that uplift rates have been constant. The I-stage that lasted from 26,000 to 4000 B.P., was interpolated to be 15,000 B.P. by *R. S. U. Smith* [1976; also unpublished guidebook, 1978]. The interpolation method itself, as pointed out by R. S. U. Smith (unpublished guidebook, 1978), contains some uncertainty. In this study, we will use the 26,000 to 4000 B.P. as the age of the I-stage of fluctuation to try to find the relation between the I-stage shorelines and some geomorphic surfaces which are offset by the fault.

North of Manly Peak Canyon, a series of alluvial features, such as debris flows, and alluvial channels and ridges, have been offset right-laterally. The amount of offset varies from 15 to 27 m (Site 5 in Figure 3). To accurately measure the offset we used a plane table and alidade to construct detailed topographic maps of the offset features. Figure 8 shows two offset alluvial ridges. The ridges are narrow and elongate and lie between two alluvial channels formed during debris flow on the surface of an alluvial fan. The fault trends about N30W. The displacement of both ridges is clearly visible. Alluvial ridge A on the eastern side of the fault trends about N10E and is relatively straight with a steeper southern slope.

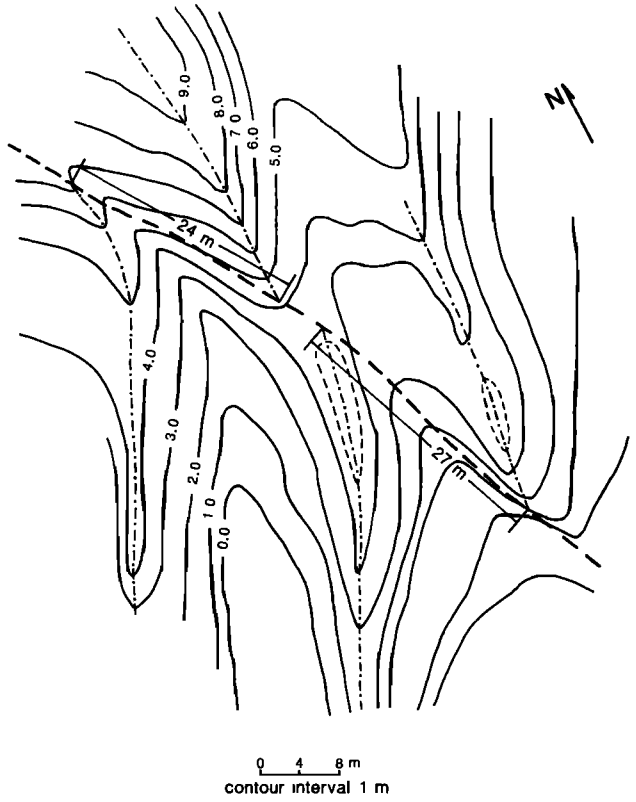

Fig. 8. Topographic contour map of alluvial ridges offset right-laterally near Manly Peak Canyon (Site 5). Thick lines represent fault scarps. Dashed lines indicate the offset ridge crests. The measured offset between A and A′ is 27 ± 4.0 m, and 24 ± 4.0 m. The elevation is arbitrary.

In most places the top of the ridge is less than one meter in width. Ridge A′ on western side of the fault has a width similar to that of ridge A, but about 6 m from the fault the trend of the ridge changes to N5–10E as it approaches the fault. The distance between ridge A and A′ along the fault gives a displacement of 27 ± 4 m (Figure 8). Alluvial ridges B and B′ are less well defined than A and A′ (Figure 8), and are offset by 24 ± 4 m.

The uncertainty of these estimates results from two sources: 1, projection of ridge lines to the fault, and 2, the post-offset erosion of the ridges. All of the four ridges are narrow and well defined. Their crests are usually 1 to 2 m wide. The projection of the ridge crests probably results in ± 2 m in uncertainty. The distance between the projection of A and B is about 3 m larger than the distance between A′ and B′ (Figure 8). This suggests some minor post-offset erosion of the ridges. This erosion may contributes another ± 2 m uncertainty to the displacement. Thus, the total uncertainty of the displacement may be as large as ± 4 m.

These offset alluvial ridges are present on an old part of the Manly Peak alluvial fan system (Qoa in Figure 9*b*) that consists of a series of debris flows, alluvial channels, and alluvial ridges. This part of the fan is no longer active; the present locus of erosion and deposition has migrated to the north (Figure 9*a*, *b*), explaining the preservation of the morphology here. This part of the fan is composed of angular cobbles, boulders, pebbles, and rock fragments. No lacustrine sediments and wave-cutting features can be found on its surface or within the constitutive material. This part of the fan is present from the level between 1500 to 1300 feet. It seems clear that the surface of this part of the fan can not have formed during the last high stand of Lake Panamint because it is several hundred feet below the lake surface. Thus, its age has to be younger than the age of the last high stand of Lake Panamint. It is clear from Figure 9*a* and 9*b* that this part of the fan (Qoa) cuts the beach platform between 1250 to 1400 feet. The same fan material may even reach below 1200 feet, the final low stand of Lake Panamint, but the modern alluvial and eolian sand obscure this relationship. The maximum age of displacement of the alluvial ridges could be determined if the age of the last high stand was known.

Various features on the lower part of Manly Peak fan (wave-cutting cliff and notches, sand and silt deposit, and beach berms) suggest that it used to be a gently inclined beach (Figure 9*a*, *b*). This beach platform was probably formed during latest period of I-stage (13,000 years ago) defined by *R. S. U. Smith* [1976; also unpublished guidebook, 1978]. The upper part of the Manly Peak alluvial fan (1200 to 1500 feet) is dominated by lacustrine sediments such as sand, silt, and rounded pebbles and cobbles. The age of the surface of the Manly Peak fan is probably younger than the age of last I-stage high stand of Lake Panamint (2040 to 1900 feet). This age, however, is not easy to estimate. The I-stage lasted from 26,000 to 4000 B.P. [*R. S. U. Smith*, 1976; also unpublished guidebook, 1978]. Based on correlation with the pluvial shoreline studies in Lake Searles *R. S. U. Smith* [1976] suggested the last low stand of Lake Panamint (about 1200 feet) was 13,000 to 12,000 years ago which gives the lower bound for the age of the last high stand of Lake Panamint. It appears to be reasonable to assume that high stands last at least 5000 years from the beginning of I-stage fluctuation, otherwise they are unlikely to create benches and to form nodose tufa. If this is so, the age of I-stage high stand could be constrained to be from 21,000 to 13,000 B.P. Thus, the maximum age of the offset alluvial ridges can be constrained to be 17,000 ± 4000 yr. Given the displacement of alluvial ridges to be 27 ± 4 m and 24 ± 4 m, the minimum latest Pleistocene and Holocene slip rate is from 1.09 to 2.38 mm/yr., or 1.74 ± 0.65 mm/yr.

The Holocene slip rate was also determined by an offset feature north of Goler Wash Canyon (Site 6 of Figure 3). The 2 m high fault scarp trends about N20W and dips to the east. A detailed plane table map shows this offset and scarp (Figure 10). The edge of an alluvial fan is offset by 37 m (Figures 10). This alluvial fan covers the top of fine-grained lacustrine sand and silt. On the western side of the fault a 0.1–0.2 m deep east-trending channel cuts through fan material and exposes underlying lacustrine sand and silt. The original edge of the fan on the western side is constrained to be within 2 m of its present position by the absence of fan material in the banks of a small channel 2 m north of the present edge. The northern edge of the fan on the eastern side of the fault has been subjected to some minor undercutting, but the modification appears to be minor because the topography is gentle and only very few erosional features such as runoff channels are present on the surface of the fan. Offset of the edge of the alluvial fan is 37 ± 4.0 m. The 4.0 m uncertainty is due to the possibility of modification of the edge of the alluvial fan.

The offset alluvial fan is composed of sediments that consist of angular cobbles and pebbles with a matrix of small

Fig. 9*a*

Fig. 9. Low-sun angle aerial photo and the interpretation of the Manly Peak Canyon alluvial fan and the fault scarps. A, low-sun angle aerial photo. B, geomorphic map of the area covered by the photo. Pbr, Paleozoic bed rocks; Qhs, Pleistocene high shorelines; Qms, Pleistocene medium shorelines; Qls, Pleistocene low shorelines, Qoa, old alluvial surface; Qya, young alluvial surface; Qal, the alluvial surfaces not part of the Manly Peak Canyon alluvial system; Qpp, present playa. Thick lines are fault scarps with ticks indicating dips of fault scarps.

pebbles and rock fragments. No lacustrine material such as tufa, sand, or silt was found within the matrix. Thus, this fan was formed after the desiccation of Lake Panamint, because the fan shows sub-arid forms rather than deltaic forms, and because the sediments contain no lacustrine material. This offset fan edge is part of a large alluvial fan from Goler Wash Canyon, which covers and cuts a well-developed gently sloping depositional lacustrine terrace between elevations of 1200 to 1400 feet between Goler Wash Canyon and Coyote Canyon (Figure 11*a*, *b*). This lacustrine terrace consists of rounded pebbles and cobbles, sand, and silt. Its surface is relative flat and gently sloping to the west. The offset fan that cuts and covers this terrace was formed when the lake surface stood below this terrace. This implies that the age of the offset fan must be younger than the age of the last high stand of Lake Panamint. The edge of the offset alluvial fan is below 1200 feet and directly covers fine grained lacustrine sand and silt which is a portion of present playa and was a portion of previous lake bottom. Therefore, the age of the offset is younger than 17,000 ± 4000 B.P., and may be younger than 13,000–12,000 B.P. For the 37 ± 4.0 m offset and 17,000 ± 4000 B.P. maximum age, the minimum Holocene slip rate is 1.57 to 3.15 mm/yr, or 2.36 ± 0.79 mm/yr.

The minimum Holocene slip rates obtained from Manly Peak Canyon and Goler Wash Canyon are 1.74 ± 0.65 mm/yr and 2.36 ± 0.79 mm/yr, respectively. The minimum rate from Goler Wash Canyon, 2.36 ± 0.79 place a tighter constraint on the true slip rate, and thus is the one used in subsequent discussion.

DISCUSSION

The studies of Holocene activity on the southern Panamint Valley fault zone motivate several important questions with regard to both the regional style of modern deformation, its corollaries for deformation in coastal California, and the

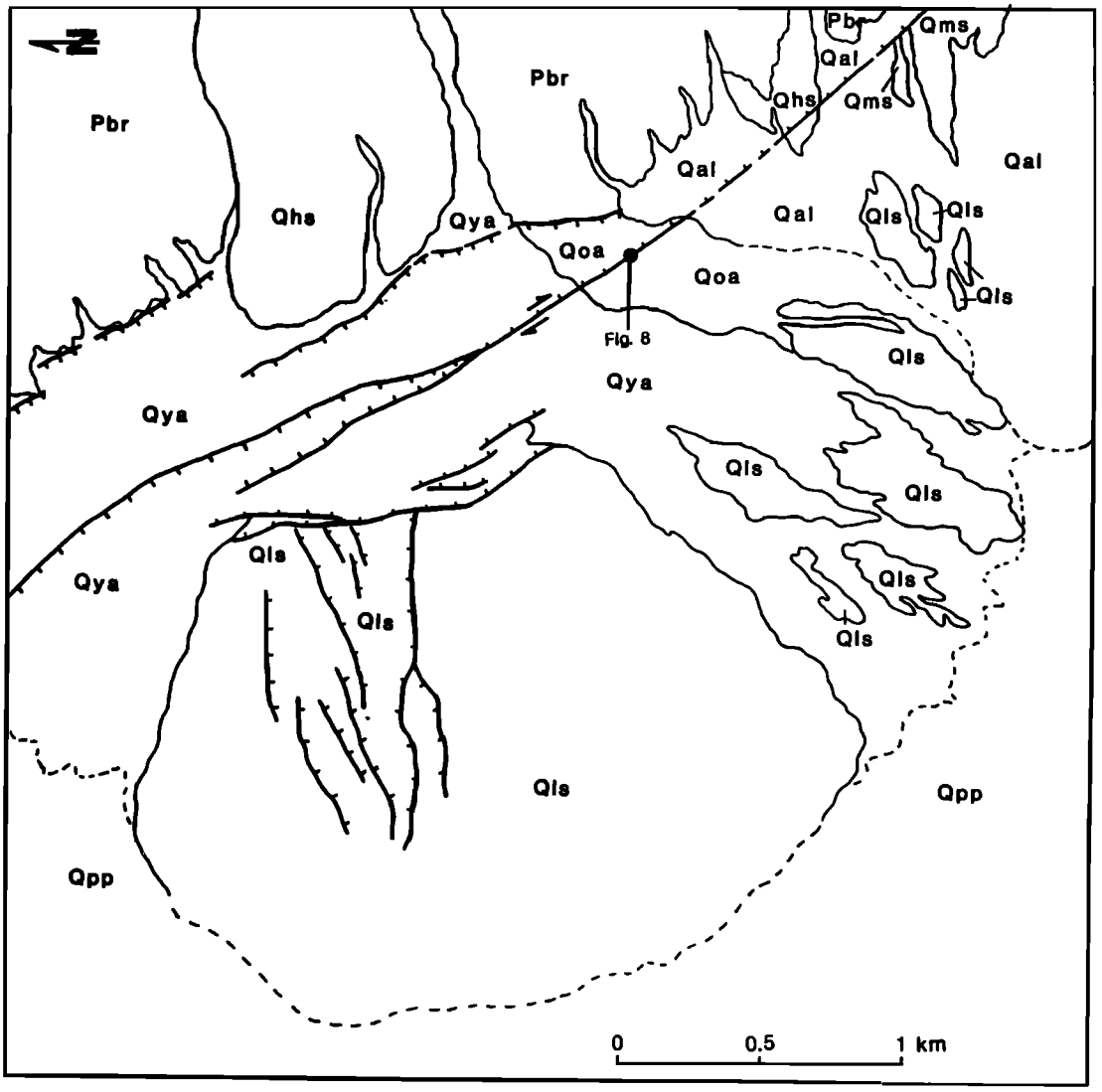

Fig. 9*b*.

local fault behavior. Although the resolution of these questions requires more work, we offer in the following sections what we hope are some reasonable speculations.

Characteristic Earthquake and the Earthquake Recurrence Interval

The characteristic earthquake model suggests that an individual fault or fault segment tends to generate essentially the same size earthquake, the so-called characteristic earthquake [*Schwartz and Coppersmith*, 1984, 1986]. Similarly, the displacement associated with each characteristic earthquake should be similar for a certain fault or fault segment. Our study suggests that the characteristic earthquake model is applicable to the southern Panamint Valley fault zone. If about 3 m right-lateral displacement is associated with the prehistoric characteristic earthquake along the southern Panamint Valley fault zone, we would expect to see right-lateral offsets in multiples of 3 m. In fact, we do observe offsets of about 6 m and 12 m at many places along the fault zone between Manly Peak Canyon and Goler Wash Canyon (Figures 3, 4 and 6). We cannot dismiss the possibility of course that the larger offsets are the product of irregular displacements. Moreover, the case for a characteristic earthquake is not unambiguous; the total slip during the last event across the Goler Wash fan may be up to 4 m (Figure 3). Nevertheless, the consistency of ~6 m (6 measurements) and ~12 m (8 measurements) offsets suggest that the Holocene activity of the fault may involve a characteristic earthquake of magnitude 6.5 to 7.2 (Ms).

The average recurrence interval may be determined from the Holocene slip rate and the amount of displacement per event. In order for the average recurrence interval to be meaningful for seismic hazard analysis, we need to satisfy three conditions: (1) Displacement is mostly co-seismic; (2) Slip rate remains constant throughout both the past and future time periods of interest, and essentially throughout the entire fault zone or fault segment; and (3) We have a reasonable expectation for the magnitude of the displacement and its consistency over the time of interest.

The first condition is supported here by the sharpness of offset features, suggesting that the offsets were abrupt and not gradual. This, plus the fact that no known example of fault creep is known in the Basin and Range Province, suggests that fault creep is probably negligible. The second

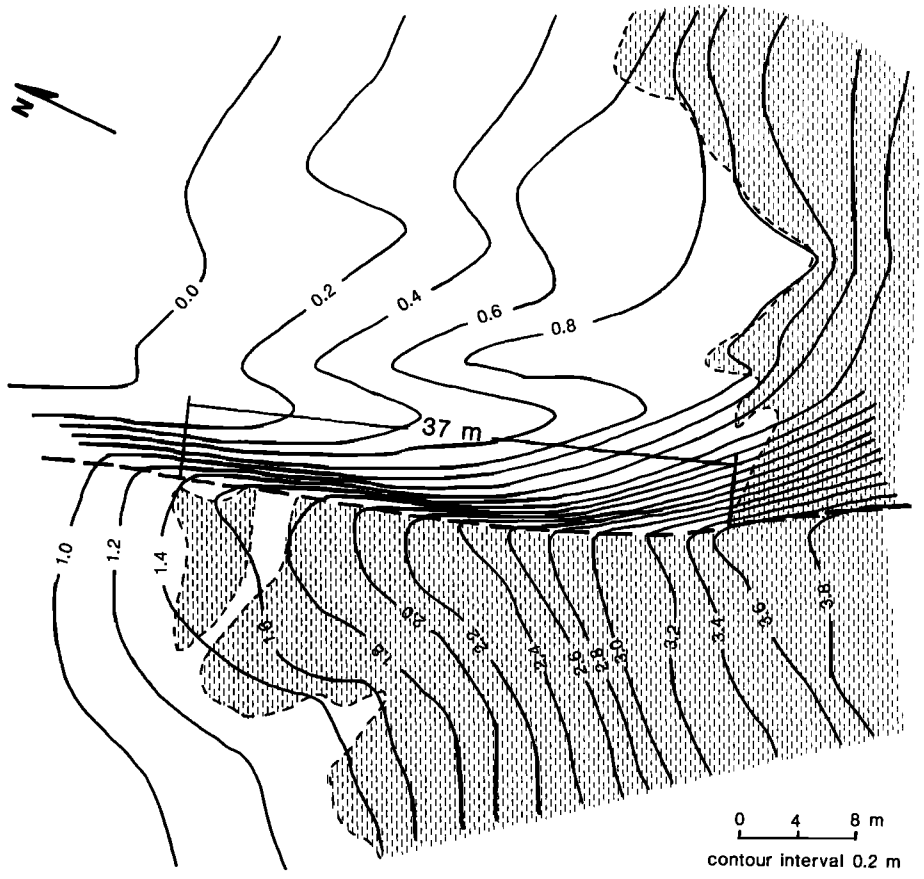

Fig. 10. Topographic contour map of offset alluvial fan near Goler Wash Canyon (Site 6). Dashed thick line indicates the fault scarp that offsets the edge of an alluvial fan. The alluvial fan is marked by the shaded area on the map. The fan covers fine grained sand and silt that probably was deposited on the lake bottom. The measured right-lateral offset is 37 ± 4.0 m. The elevation is arbitrary.

condition is reasonably satisfied since we know the Pliocene time-averaged slip rate of the linked Hunter Mountain fault, 2–2.7 mm/yr, is similar to that of the southern Panamint Valley fault zone, 2.36 ± 0.79 mm/yr. The third condition is satisfied if the characteristic earthquake model is appropriate for this fault zone, which we have discussed above. Setting the Holocene slip rate at 2.36 ± 0.79 mm/yr and the characteristic event at 3.2 ± 0.5 m, the average recurrence interval during the Holocene is between 860 and 2360 years.

The similarity of the very long-term slip rate for the Hunter Mountain fault (2–2.7 mm/yr, 4 Ma, Burchfiel et al., 1987) and the long-term minimum slip rate for the Panamint Valley fault (2.36 ± 0.79 mm/yr, 17,000 ± 4000 yr) is interesting. Given this similarity one may argue that the rate of deformation has been similar over the past 4 million years. If we go one step further, with the characteristic earthquake model, these data imply a regular earthquake recurrence interval or temporal regularity at least through Holocene time. This argument is consistent with observations by *Wallace* [1984, 1987], *Schwartz* [1988], and *Coppersmith* [1989] who point out that paleoseismicity in the Basin and Range Province appears to show considerable temporal clustering that may extend back over several millions of years. However, the slip rate on a fault may change regularly or irregularly with time [*Knuefer*, 1987; *Machette*, 1987]. Since we have no information about slip rates time-averaged over intervals between 17,000 years and 4 million years, any argument about such long-term clustering is highly speculative.

Implications for the Style of Deformation in the Death Valley Extensional Region

The mechanism of extension in the Death Valley region has been characterized as a series of pull-apart basins, whereby the basins are opening obliquely and are kinematically linked to strike-slip faults [*Burchfiel and Stewart*, 1966], and which may be associated with shallow (<5 km) low-angle normal faults [e.g., *Burchfiel et al.*, 1987; *MIT Field Geophysics Course and Biehler*, 1987]. If Panamint Valley is also a pull-apart basin then the slip vector or opening direction should be given by the N60°W—trending, dextral strike-slip Hunter Mountain fault (Fig. 2). Our results combined with those of *R. S. U. Smith* [1979] show the minimum horizontal slip vector for the southern Panamint Valley fault to be oriented toward ~N35W. If this slip vector is representative of that for whole Panamint Valley fault system, then the pull-apart origin of Panamint valley is only partially satisfied. That is, since the two slip vectors differ by ~25°, the kinematic link between the Panamint Valley fault and the Hunter Mountain fault is not simple, and some deformation must be accommodated off the main fault systems [*Ellis et al.*, 1989].

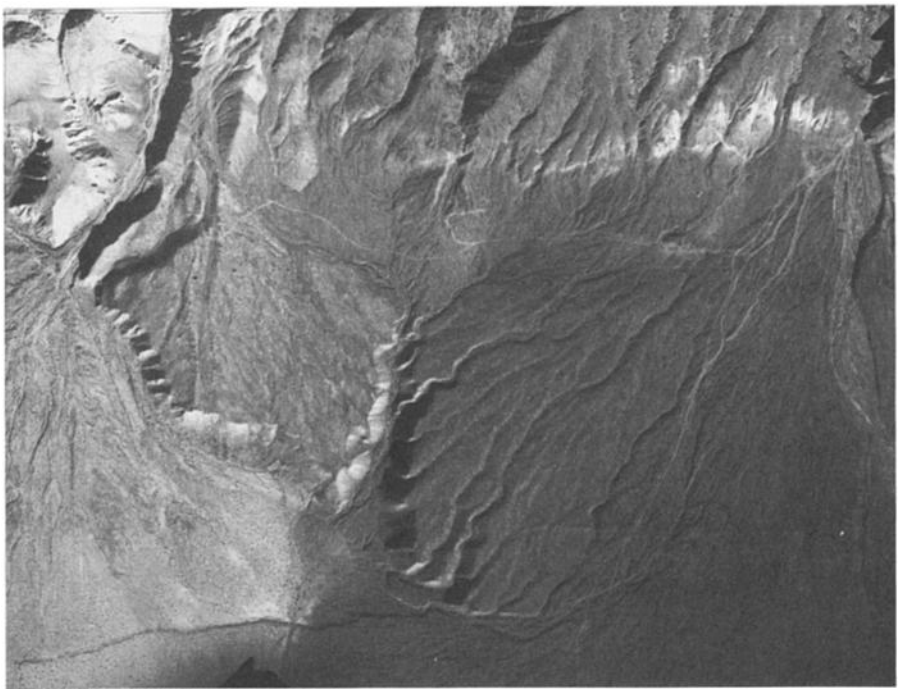

Fig. 11*a*

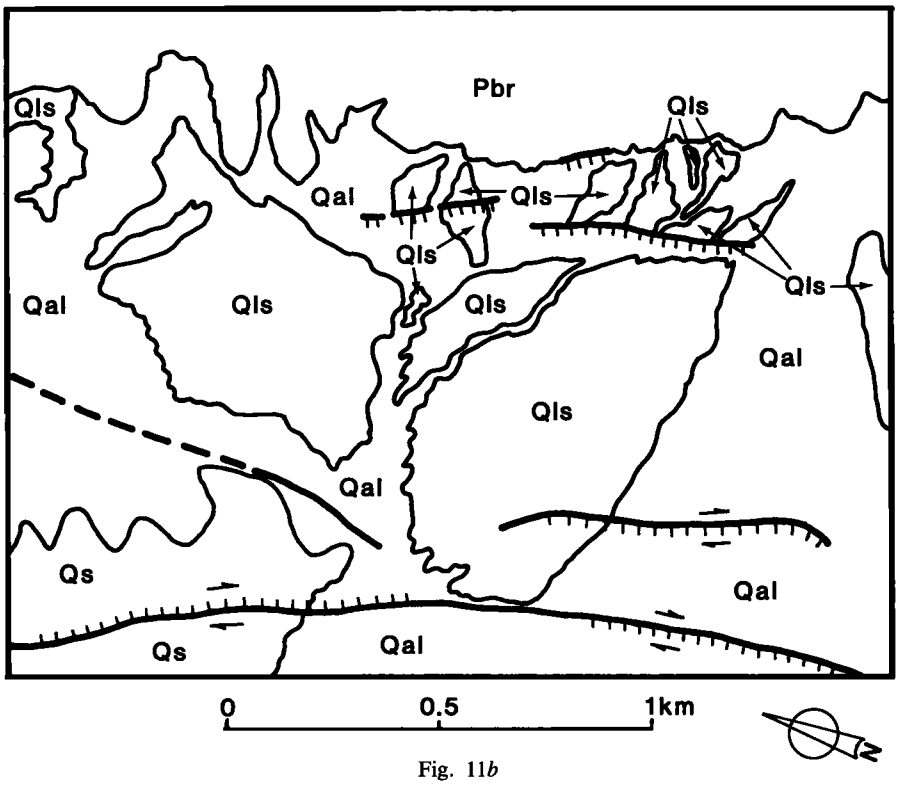

Fig. 11*b*

Fig. 11. Low-sun angle aerial photo (A) and interpretation of geomorphic features and fault scarps (B). Pbr is Paleozoic bed rock, Qls is late Pleistocene low shorelines, Qal is an alluvial fan that cuts and covers the shoreline, and Qs is Holocene sand. Thick lines represent fault scarps and ticks indicate dips of those scarps.

Our studies also suggest that the oblique-slip currently occurring on the Panamint Valley fault zone is partitioned between strike-slip and dip-slip faults, and that dip-slip faults are commonly restricted to the range front while strike-slip faults are off the range front. This style appears to characterize lake Cenozoic and modern deformation in the entire Death Valley Extensional Region. In Owens Valley, the west-dipping Sierra Nevada mountain-front fault shows basically normal faulting, and the middle valley fault shows strike-slip motion (Slemmons et al., manuscript in preparation, 1990; Beanland and Clark, manuscript in preparation, 1990). The 1872 Owens Valley earthquake occurred along

the middle valley fault and was associated with 110 km rupture with an average right-slip of 6 m and a vertical slip of 1 m [*de Polo et al.*, 1989]. The northern Death Valley fault crops out along the east-central part of the valley floor and is essentially strike-slip [*Brogan*, 1979], while the mountain-front faults along both sides of Death Valley are basically normal faults. Further east in Pahrump Valley, the active deformation in the middle valley appears to be characterized by strike-slip motion.

We do not offer any explanation for this partitioning, except to suggest that it may be related to the complex, three-dimensional modern deformation of the southern Great Basin. Such complex deformations (that involve, for example, rigid-body rotations) require a number of linearly-independent slip systems, which corresponds to a number of linearly-independent, differently oriented fault systems, to maintain strain compatibility over the region.

Steady State Displacement Vectors in the Southern Great Basin

In this section, we discuss the evaluation of steady-state displacement rates and their orientations in the context of plate tectonic models of the Basin and Range and coastal California. Our results shed some light on reasonably long-term time-averaged displacement rates (~2.36 mm/yr over ~17,000 years) that appear to be representative of the very-long term displacement rate (2–2.7 mm/yr over 4 million years). Additionally, our results suggest that the displacement vector in the southern Great Basin is NW to NNW, rather than WNW as preferred by *Minster and Jordan* [1987] and *Jordan and Minster* [1988]. This has important consequences for deformation in the coastal California region.

Plate tectonic models generally yield a relative motion vector between the North American and Pacific plates of ~56 ± 3 mm/yr in a direction N35°W ± 2° (RM2 of *Minster and Jordan* [1978]) and ~49 ± 3 mm/yr in a direction N34°W (Nuvel 1 of *DeMets et al.* [1987]). Both of these vectors correspond to 3 Ma time-averages. Slip on the central California section of the San Andreas fault is derived from two offset geomorphic features whose maximum age is estimated to be ~3,700 years and 13,250 years [*Sieh and Jahns*, 1984]. Thus, the San Andreas discrepancy vector suffers from being the resultant of two different time-averaged vectors, one over 3 Ma and one over Holocene time.

The San Andreas discrepancy is normally decomposed into Basin and Range and coastal California components (Figure 12). Since much of the deformation in coastal California is offshore and not easily determined, evaluation of the San Andreas discrepancy and of the active deformation within the Basin and Range are important constraints on the coastal California component. We need to know either the very long-term slip rate (several Ma) on the San Andreas fault or the long-term (several ka) relative plate motion vector in order to properly evaluate the San Andreas discrepancy. Our results, although restricted to a relatively small area, carry some implications for the very long-term slip rate of the San Andreas fault. The southern Panamint Valley fault appears to be slipping at a rate of 2.36 ± 0.79 mm/yr time-averaged over ~17,000 years, which is essentially the same as the ~4 Ma slip-rate of 2–2.7 mm/yr for the linked Hunter Mountain fault [*Burchfiel et al.*, 1987]. This suggests that the southern Great Basin has undergone fairly constant extension over the last 4 Ma and that 17,000 years is a representative time sample over which to estimate very long-term slip rates. If this is also true for the entire plate boundary tectonics of western North America, then the Holocene slip-rate of the San Andreas may well be representative of its very long-term slip rate. The second constraint on coastal California deformation is that within the Basin and Range.

Deformation in the Basin and Range province is estimated through VLBI (Very Long Baseline Interferometry) data [e.g., *Minster and Jordan*, 1987; *Jordan and Minster*, 1988], which is currently time-averaged over about 15 years. VLBI data alone yield a displacement vector of the Sierra Nevada block relative to the Colorado Plateau of ~9 ± 3.9 mm/yr in a direction N48°W ± 17° [*Minster and Jordan*, 1987]. Minster and Jordan's preferred displacement vector, 9.7 ± 2 mm/yr in a direction N56°W ± 10°, is derived by incorporating geological data from the Basin and Range that alone shows the direction of extension to be ~N60°W [*Zoback and Zoback*, 1980]. It is difficult to have much confidence in the geologically-derived direction simply because the various features measured by *Zoback and Zoback* [1980] represent different time-averaged results, but also because these features yield a mixture of extension and displacement estimates, and the relationship between strain and displacement is not always simple.

The displacement vector for the Basin and Range can be determined most efficiently by evaluating the steady state displacements associated with the large active faults. Steady state displacement rates are generally not available from the seismic record, which is well known to be too short and too noisy [e.g. Ambraseys, 1989]. For example, the seismic record for the southern Great Basin shows the displacement rate to be either 3.5 mm/yr or 29.2 mm/yr, the latter including the 1872, Owens Valley, M ~8.3, earthquake, the former not [*Eddington et al.*, 1987]. Steady state displacement rates are more likely to be obtained through paleoseismological analyses of active faults. Unfortunately such analyses are still rare, and we can only offer a mixture of quantitative and qualitative arguments for the southern Great Basin.

We can estimate the displacement vector in the Panamint Valley area by noting the kinematics of the linked Hunter Mountain strike slip fault and the Panamint Valley fault. We have shown that the southern Panamint Valley fault is predominantly strike-slip [see *R. S. U. Smith*, 1979], and the strike-slip nature is clearly evident along the northern section of the fault, toward the bend between the Hunter Mountain fault and the Panamint Valley fault [*Burchfiel et al.*, 1987; *Ellis et al.*, 1989; *Hodges et al.*, 1989]. The total displacement vector probably lies between the orientations of these two faults, that is, between N60°W and N20°W, consistent with analyses of VLBI data [*Minister and Jordan*, 1987; *Argus et al.*, 1988].

We can further estimate the displacement vector for the southern Great Basin through the kinematics of the major active faults within the region (Figure 1). The slip rate along the Owens Valley system, is 0.7–2.2 mm/yr [*Lubetkin and Clark*, 1988]. There is little other quantitative slip rate data at this latitude, although we should expect the Death Valley system (judging by the geomorphology) to be slipping at a rate of at least 2 mm/yr. There are probably smaller amounts of slip occurring further east in Pahrump Valley and within southern Nevada and southwestern Utah, although the

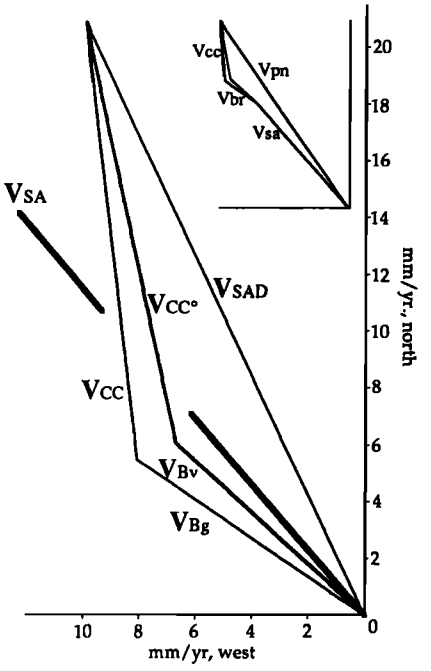

Fig. 12. Components of the relative PAC-NOAM plate motion vector: San Andreas discrepancy, V_{SAD}; Geologically-constrained Basin and Range, V_{Bg}; VLBI Basin and Range and our preference, V_{Bv}; currently preferred Coastal California model C of *Minster and Jordan* [1987], V_{CC}; Coastal California preferred in this paper and model B of Minster and Jordan, $V_{CC°}$. The bold line marks the direction of the San Andreas slip vector, V_{SA}; and the inset shows Minster and Jordan's relative plate motion vector and its components.

amount is unknown. Thus, the long-term slip rate of the southern Great Basin is probably a minimum of 8 mm/yr in a direction between NW and NNW (Figure 12). We realize that far more data are required if we are to perform a quantitative regional integration of the deformation, and we offer this result as speculation.

If the total displacement vector for the southern Great Basin is closer to the VLBI model result of N48°W (rather than the geologically-constrained N56°W) and, further, if this is true also for the whole Basin and Range, then the coastal California component will be closer to model B of *Minster and Jordan* [1987]. That is, the coastal California displacement vector will consist of ~13 mm/yr parallel, and ~6.5 mm/yr perpendicular (Figure 12), to the San Andreas fault [*Minster and Jordan*, 1987].

Conclusions

A 25 km-long, fresh zone of fault scarps along the southern Panamint valley fault zone is recognized as the surface rupture zone associated with the most recent prehistoric earthquake. The predominant sense of motion is right-lateral displacement. The offset associated with the most recent prehistoric event is 3.2 ± 0.5 m. A number of large offsets in range of 6–7 m and 12 m are also observed, and at two places offsets of 27 ± 4 m and 37 ± 4 m have been measured. The ages of these largest offsets is estimated by the relation between late Pleistocene shorelines and alluvial fan features. From these data the rate of Holocene slip along the southern Panamint Valley fault zone is estimated to be 2.36 ± 0.69 mm/yr. Since the cumulative offsets along the fault zone are commonly multiples of the single-event offset (about 3 m), the fault zone may be associated with a characteristic earthquake, which we estimate to be in the magnitude range 6.5 to 7.2 (Ms). Given such a characteristic earthquake, the recurrence interval is between 860 and 2360 years.

The Holocene slip rate appears to be similar to the 4 million year slip rate of 2–2.7 mm/yr (determined from the Hunter Mountain fault), which we suggest reflects the relatively constant tectonics in this region over the last 4 million years. This in turn supports the San Andreas discrepancy in that the Holocene slip rate of the San Andreas fault probably represents its mid-Pliocene time-averaged slip rate. The total slip vector of the southern Panamint Valley fault system is oriented toward ~N35°W, making this a predominantly strike-slip fault. Given the N60°W-trending strike-slip Hunter Mountain fault, we suggest that the displacement vector for the southern Great Basin is toward the NW, consistent with results from VLBI data, rather than WNW as determined by combining VLBI and geological data. A corollary states that the coastal California deformation component involves, respectively, less shortening and more strike-slip displacement perpendicular and parallel to the San Andreas fault than is currently proposed.

Acknowledgments. We are grateful to the careful criticisms by Kevin Coppersmith, Sally McGill, and Malcolm Clark, which greatly improved the paper. This work was funded by the State of Nevada, Nuclear Waste Projects Office. PZ is grateful to Dr. L. Hsu of UNR for generously providing office space during his stay in Reno. We are also grateful to Eugene Schweig III (Center for Earthquake Research and Information, MSU) and Clark Burchfiel (MIT) for information concerning the age of the late Neogene basalts in the northern Panamint Valley area.

References

Ambraseys, N. N., Temporary seismic quiescence: SE Turkey, *Geophys. J. R. Astron. Soc.*, *96*, 311–331, 1989.

Argus, D. F., and R. G. Gordon, Sierra Nevada-North America motion from VLBI and paleomagnetic data: Implications for the kinematics of the Basin and Range, Colorado Plateau, and California Coastal Ranges (abstract), *Eos Trans. AGU*, *69*, 1418, 1988.

Bell, J. W., D. B. Slemmons, and R. E. Wallace, Roadlog: Reno to Dixie Valley-Fairview Peak earthquake areas, field trip 18: *Geological Society of America*, 1984 Annual Meeting, Western Geological Excursions, *4*, 425–472, 1984.

Brogan, G. E., Late Quaternary faulting along the Death Valley—Furnace Creek fault system, California and Nevada, *Rep. 14-08-0001-17801*, U.S. Geol. Surv., Menlo Park, Calif., 1979.

Burchfiel, B. C., and J. H. Steward, "Pull-apart" origin of the central segment of Death Valley, California, *Bull. Geol. Soc. Am.*, *8*, 439–442, 1966.

Burchfiel, B. C., K. V. Hodges, and L. H. Royden, Geology of Panamint Valley—Saline Valley pull-apart system, California: Palinspastic evidence for low-angle geometry of a Neogene range-bounding fault, *J. Geophys. Res.*, *92*, 10,422–10,426, 1987.

Coppersmith, K. J., On spatial and temporal clustering of paleosiesmic events, *Seismol. Res. Lett.*, *59*, 299–230, 1989.

DeMets, C., R. G. Gordon, S. Stein, and D. F. Argus, A revised estimate of Pacific-North American motion and implications for western North America plate boundary zone tectonics, *Geophys. Res. Lett.*, *14*, 911–914, 1987.

dePolo, C. M., D. G. Clark, and D. B. Slemmons, Historical Basin and Range Province surface faulting and fault segmentation, *U.S. Geol. Sur. Open File Rep.*, *89-315*, 131–162, 1989.

Eddington, P. K., R. B. Smith, and C. Renggli, Kinematics of an extending lithosphere, the U.S. Cordillera, *Geol. Soc. Spec. Publ.*, *28*, 371–392, 1987.

Ellis, M. A., P. Bodin, and J. G. Anderson, Geological and geophysical evidence for the existence of low-angle normal faults (abstract), paper presented at 20th Geological Society of American Annual Meeting, Geol. Soc. Am. Boulder, Colo., 1988.

Ellis, M. A., P. Zhang, D. B. Slemmons, Active Tectonics of the Southern Panamint Valley: Implications for the Proposed Low-Angle Normal Fault under Northern Panamint Valley (abstract), *Eos Trans. AGU, 70*, 465, 1989.

Hall, W. E., Geology of the Panamint Butte quadrangle, Inyo County, California, *U.S. Geol. Surv. Bull., 1299*, 67 pp., 1971.

Hileman, J. A., Allen, C. R., and J. M. Nordquist, Seismicity of the southern California region: Pasadena, California, report, Calif. Inst. Technol. Seismol. Lab., Pasadena, 1973.

Hodges, K. V., L. W. McKenna, J. Stock, J. Knapp, L. Page, K. Sternlof, D. Silverberg, G. Wust, and J. D. Walker, Evolution of extensional basins and Basin and Range topography west of Death Valley, California, *Tectonics, 8*, 453–467, 1989.

Jones, C. H., Is extension in Death Valley accommodated by thinning of the mantle lithosphere beneath the Sierra Nevada, California?, *Tectonics, 6*, 449–473, 1987.

Jordan, T. H. and J. B. Minster, Measuring crustal deformation in the American West, *Sci. Am., 256*, 48–58, 1988.

Knuepfer, P. L. K., Change in Holocene slip rate in strike-slip environment, *U.S. Geol. Surv. Open File Rep. 87-673*, 249–261, 1987.

Larsen, R. W., Chronology of Late Cenozoic basaltic volcanism: The tectonic implications along a segment of the Sierra Nevada and Basin and Range Province, Ph. D. thesis, 95 pp., Brigham Young Univ., Provo, Utah, 1979.

Lubetkin, L. K. C., and M. M. Clark, Late Quaternary activity along the Lone Pine fault, eastern California, *Bull. Geol. Soc. Am., 100*, 755–766, 1988.

Machette, M. N., Change in long-term versus short-term slip rates in an extensional environment, *U.S. Geol. Surv. Open File Rep. 87-673*, 228–238, 1987.

Minster, J. B., and T. H. Jordan, Vector constraints on western U.S. deformation from space geodesy, neotectonics, and plate tectonics, *J. Geophys. Res., 92*, 4798–4804, 1987.

MIT Field Geophysics Course, and S. Biehler, A geophysical investigation of the northern Panamint Valley, Inyo County, California: evidence for possible low-angle normal faulting at shallow depth in the crust, *J. Geophys. Res., 92*, 10,427–10,441, 1987.

Noble, L. F., Structural features of the Virgin Spring area, Death Valley, California, *Bull. Geol. Soc. Am., 52*, 941–1000, 1941.

Real, C. R., T. R. Toppozada, and D. L. Parke, Earthquake epicenter map of California, Map Sheet 39, Calif. Div. Mines and Geol., Sacramento, 1978.

Richter, C. F., Elementary Seismology, p. 768 W. H. Freeman, New York, 1958.

Sawyer, L. T., Late Holocene Paleoseismicity of the northern Death Valley fault system, Fish Lake Valley, Nevada, Late Cenozoic Evolution of the Southern Great Basin, edited by M. A. Ellis, *Open File Rep. 89-1*, pp. 63–78, Nev. Bur. of Mines and Geol., Reno, Nev., 1989.

Schwartz, D. P., Geologic characterization of seismic sources moving into the 1990s, American Society of Civil Engineers, *Geotech. Spec. Publ. 20*, 1–42, 1988.

Schwartz, D. P., and K. J. Coppersmith, Fault behavior and characteristic earthquakes: examples from the Wasatch and San Andreas Fault zones, *J. Geophys. Res., 89*, 5681–5698, 1984.

Schwartz, D. P., and K. J. Coppersmith, Seismic hazard: New trends in analysis using geologic data, in *Active Tectonics*, pp. 215–230, National Academy Press, Washington, D. C., 1986.

Schweig, E. S., III, Neogene tectonics and Paleogeography of the southwestern Great Basin, California, Ph.D. thesis, Stanford Univ., Palo Alto, California, 1985.

Schweig, E. S., III, Basin and Range tectonics in Darwin Plateau, southwestern Great Basin, California, *Geol. Soc. Am. Bull., 101*, 652–662, 1989.

Sieh, K. E., Slip along the San Andreas fault associated with the great 1857 earthquake, *Bull. Seismol. Soc. Am., 68*, 1421–1448, 1978.

Sieh, K. E., and R. Jahns, Holocene activity of the San Andreas fault at Wallace Creek, California, *Geol. Soc. Am. Bull., 95*, 883–896, 1984.

Slemmoms, D. B., Geological effects of the Dixie Valley—Fairview Peak, Nevada, earthquakes of December 16, 1954, *Bull. Seismol. Soc. Am., 47*, 353–375, 1957.

Slemmons, D. B., P. Bordin, and X. Zhang, Determination of earthquake size for active faults, in *Proceedings of the International Seminar on Seismic Zonation*, p. 157–169, State Seismological Bureau of China, Guangzhou, China, 1988.

Slemmons, D. B., P. Zhang, and F. Mao, Geometry and displacement of surface rupture zone associated with the 1954 Fairview Peak, Nevada, earthquake, *Seismol. Res. Lett., 60*, 30, 1989.

Smith, R. B., Seismicity, crustal structure, and intraplate tectonics of the interior of the western Cordillera, *Geol. Soc. Am., Mem., 152*, 111–144, 1978.

Smith, R. S. U., Late Quaternary pluvial and tectonic history of Panamint Valley, Inyo and San Bernardino counties, California, Ph.D. dissertation, Calif. Inst. Technol., 1976.

Smith, R. S. U., Holocene offset and seismicity along the Panamint Valley fault zone, western Basin and Range Province, California, *Tectonophysics, 52*, 411–415, 1979.

Sternlof, K. R., Structural style and kinematic history of the active Panamint-Saline extensional system, Inyo County, California, M.S. theses, Mass. Inst. of Technol., Cambridge, 1988.

Stewart, J. H., Basin-range structure in western North America: A review, *Mem. Geol. Soc. Am., 152*, 1–31, 1978.

Stewart, J. H., Extensional tectonics in the Death Valley area, California: Transport of the Panamint Range structural block 80 km northward, *Geology, 11*, 153–157, 1983.

Walker, J. D., and D. S. Coleman, Correlation of Mio-Pliocene rocks of the northern Panamint Mountains and Darwin Plateau: implications for normal fault development and the opening of Panamint Valley, *Geol. Soc. Am. Abstr. Programs, 19*, 878, 1987.

Wallace, R. E., Earthquake recurrence intervals on the San Andreas fault, *Geol. Soc. Am. Bull., 81*, 2875–2890, 1970.

Wallace, R. E., Patterns and timing of late Quaternary faulting in the Great Basin Province and relation to some regional tectonic features, *J. Geophys. Res., 89*, 5763–5769, 1984.

Wallace, R. E., Grouping and migration of surface faulting and variation in slip rate on faults in the Great Basin Province, *Bull. Seismol. Soc. Am., 77*, 868–876, 1987.

Weldon, R. J., and K. E. Sieh, Holocene rate of slip and tentative recurrence interval for large earthquakes on the San Andreas fault, Cajon Pass, southern California, *Geol. Soc. Am. Bull., 96*, 793–812, 1985.

Wernicke, B. P., J. K. Snow, and J. D. Walker, Correlation of early Mesozoic thrusts in the southern Great Basin and their possible indication of 250–300 km of Neogene crustal extension, in *The extended Land, Geological Journeys in the southern Basin and Range*, edited by D. L. Weide and M. L. Faber, pp. 255–269, Cordilleran Section, Geological Society of America, Boulder, Colo., 1988*a*.

Wernicke, B. P., G. J. Axen, and J. K. Snow, Basin and Range extensional tectonics at latitude of Las Vegas, Nevada, *Bull. Geol. Soc. Am., 100*, 1738–1757, 1988*b*.

Wernicke, B. P., J. K. Snow, G. J. Axen, B. C. Burchfiel, K. V. Hodges, J. D. Walker and P. L. Guth, Extensional tectonics in the Basin and Range Province between the Southern Sierra Nevada and the Colorado Plateau, 28th Intl. Geol. Cong., Field Trip Guideb. T138, Moscow, 1989.

Zhang, W., D. Jiao, P. Zhang, P. Molnar, B. C. Burchfiel, Q. Deng, and Y. Wang, Displacement along the Haiyuan fault associated with the great 1920 Haiyuan, China, earthquake, *Bull. Seismol. Soc. Am., 77*, 117–131, 1987.

Zhang, P., P. Molnar, B. C. Burchfiel, L. Royden, Y. Wang, Q. Deng, F. Song, W. Zhang, and D. Jiao, Bounds on the Holocene slip rate of the Haiyuan fault, north-central China, *Quat. Res. N. Y., 30*, 151–164, 1988.

Zhang, P., F. Mao, and D. B. Slemmons, Geometry and displacement of surface rupture zone associated with the 1954 Dixie Valley, Nevada, earthquake, *Seismol. Res. Lett., 60*, 30, 1989.

Zoback, M. L., and M. D. Zoback, State of stress in the conterminous United States, *J. Geophys. Res., 85*, 6113–6156, 1980.

M. Ellis, F. Mao, D. B. Slemmons, and P. Zhang, Center for Neotectonic Studies, Mackay School of Mines, University of Nevada, Reno, NV 89557

(Received April 12, 1989;
revised September 7, 1989;
accepted September 14, 1989.)